

Influence of autoionisation and predissociation on the photoelectron parameters in HBr

H Lefebvre-Brion[†], M Salzmann[‡], H-W Klausing[‡], M Müller[‡],
N Böwering[‡] and U Heinzmann[‡]

[†] Laboratoire de Photophysique Moléculaire, Bâtiment 213, Université de Paris-Sud, 91405 Orsay, France

[‡] Universität Bielefeld, Fakultät für Physik, D-4800 Bielefeld and Fritz-Haber-Institut der MPG, D-1000 Berlin 33, Federal Republic of Germany

Received 5 July 1989

Abstract. The photoionisation spectrum of HBr is strongly influenced in the 100-85 nm wavelength range by the autoionisation of Rydberg series converging to the $A^2\Sigma^+$ ionic state. These Rydberg series are also partly predissociated. Using a unified multichannel quantum-defect theory treatment of autoionisation and predissociation processes, both the photoionisation and photodissociation cross sections are calculated. The photodissociation cross section is predicted to be 10 times larger than for HCl, i.e. about 10 Mb. The photoelectron angular distribution parameter β is predicted and the influence of predissociation on its value is pointed out. The spin-polarisation parameter A (or \bar{P}) is calculated. It shows oscillatory structure related to the autoionisation of the $^1\Pi$ states. Using circularly polarised synchrotron radiation, this parameter has been measured for both fine-structure states $HBr^+ X^2\Pi_{3/2}$ ($v=0$) and $X^2\Pi_{1/2}$ ($v=0$). The agreement between calculated and measured values is relatively good.

1. Introduction

The photoionisation spectrum of HBr presents particular interest because both theoretical calculations and experiments can be readily performed for this molecule. Another reason for interest is that the ground state $X^2\Pi$ of the ion has a large spin-orbit splitting (2651 cm^{-1}). This facilitates measurements on the spin-polarisation parameters of the photoelectron, which require separation of the fine-structure components. The energy region between the $^2\Pi_{3/2}$ and $^2\Pi_{1/2}$ ionisation thresholds was previously investigated and good agreement between theory and experiment was obtained for the spin-orbit autoionisation structure (Lefebvre-Brion *et al* 1986).

In this paper, we investigate the wavelength region above the $^2\Pi$ thresholds between 100 and 85 nm, which is dominated by autoionisation resonances belonging to Rydberg series converging to the $A^2\Sigma^+$ excited state of HBr^+ . In HCl, the corresponding autoionisation features were studied previously and comparison between theory and experiment yielded an assignment for these peaks (Lefebvre-Brion *et al* 1988). More recently, the photodissociation cross section for HCl was measured in this same energy region (White *et al* 1987, Frohlich *et al* 1989). A theoretical treatment of both autoionisation and predissociation processes was made and it was shown that the $^1\Pi$ states are autoionised and the $^1\Sigma^+$ states are preferentially predissociated (Lefebvre-Brion and Keller 1989).

In molecular photoionisation, measurements of the photoelectron spin-polarisation parameter A (also denoted \bar{P}) were carried out previously for CO_2 , N_2O and CH_3Br (Heinzmann *et al* 1980, 1981) for the spin-orbit autoionisation region, and for HI in the range above the $^2\Pi$ thresholds (Böwering *et al* 1988). The spin-polarisation data for HI show a strong variation due to electronic autoionisation (Böwering *et al* 1989). A general formalism within the non-relativistic theory for the spin polarisation of the photoelectrons from diatomic molecules was derived by Cherepkov (1981) and calculations have been reported for HI and HBr (Raseev *et al* 1987) without including the electronic autoionisation.

For HBr, the absorption spectrum was analysed by Terwilliger and Smith (1974, 1975) and the photoionisation spectrum was reported briefly (Dehmer and Chupka 1978). We present here both a theoretical study of the HBr photoionisation spectrum and constant-ionic-state (CIS) photoelectron measurements. In § 2 the experimental apparatus is described. In § 3 the background of the theory is reviewed and finally in § 4 the experimental and theoretical results for the photoionisation cross section and for the spin-polarisation parameter A (or \bar{P}) of the photoelectron are compared. Predictions are made for the photodissociation cross section and for the angular asymmetry parameter β .

2. Experimental details

The photoelectron spin-polarisation parameter A (or \bar{P}) was measured in the wavelength region of 100–85 nm by performing angle- and spin-resolved photoelectron spectroscopy. The experiment was carried out with circularly polarised synchrotron radiation emitted out of the plane of the storage ring BESSY with an apparatus described in detail previously (Heckenkamp *et al* 1986). Briefly, an effusive molecular beam of HBr (99.8% purity) is crossed by vacuum-ultraviolet radiation at the exit slit of a 6.5 m normal-incidence monochromator (Schäfers *et al* 1986). A liquid-nitrogen cold trap is used to freeze the gas after crossing of the excitation region; the background pressure inside the vacuum chamber is less than 6×10^{-5} mbar. The photoelectrons emitted at reaction angle θ are energy-analysed by a rotatable hemispherical spectrometer (Jost 1979) with an energy resolution of $\Delta E = 100$ meV. For subsequent spin analysis, the electrons are accelerated to 100 keV and the transverse electron spin polarisation is measured in a Mott detector. (Two gold foils with different thicknesses and values of the Sherman function of -0.21 and -0.23 , respectively, were used.) The spin-polarisation parameter A (characterising the component $A(\theta)$ of the spin-polarisation vector parallel to the photon polarisation) can be obtained directly from measurements at the magic angle, $\theta_m = 54.7^\circ$, using left- or right-handed circularly polarised light and taking into account the degree of circular polarisation of $|P_{\text{circ}}| = (92 \pm 3)\%$.

Photoelectron spectra taken in the wavelength region examined here showed the spin-orbit split final ionic states $\text{HBr}^+ \text{X } ^2\Pi_{3/2} (v=0)$ and $\text{X } ^2\Pi_{1/2} (v=0)$ as well as several vibrationally excited peaks, which were about 10 times less intense. Since the value of the spin-orbit splitting is close to the vibrational spacing for these states (Huber and Herzberg 1979) however, peaks belonging to $^2\Pi_{1/2} (v)$ and $^3\Pi_{3/2} (v+1)$ could not be resolved. Therefore, the measurements were restricted to photoelectrons corresponding to final ionic states with $v=0$. Separate CIS measurements of the relative partial photoionisation cross section for both spin-orbit states indicated nearly identical autoionisation peaks and an almost constant branching ratio. The structures observed

were in close agreement with the total photoionisation spectrum of Dehmer and Chupka (1978).

The data obtained for the wavelength dependence of the spin-polarisation parameter A were taken in first order of the monochromator ($\Delta\lambda = 0.4$ nm) for the final ionic states $\text{HBr}^+ \text{X } ^2\Pi_{3/2} (v=0)$ and $\text{X } ^2\Pi_{1/2} (v=0)$ (denoted $A(1/2)$ and $A(3/2)$ respectively) and are shown in figure 1. The data were accumulated at the peak and valley positions of the autoionisation structures of the partial cross sections. As seen in figure 1, a strong variation in both $A(1/2)$ and $A(3/2)$ due to autoionisation is observed. In particular, a decrease to small absolute values of the polarisation occurs in the region of 90–95 nm. The results might be affected by instrumental resolution. However, two data points for $A(3/2)$ at 91.2 and 90.75 nm taken with higher resolution in second order of the monochromator were found to be in agreement with the results obtained in first order. This shows that the influence of the limited resolution is not too severe. In general, the data obtained at the same photon energy were found to be in accordance with the non-relativistic relationship (Cherepkov 1981), valid in pure Hund's case (a):

$$A(1/2) = -A(3/2). \quad (1)$$

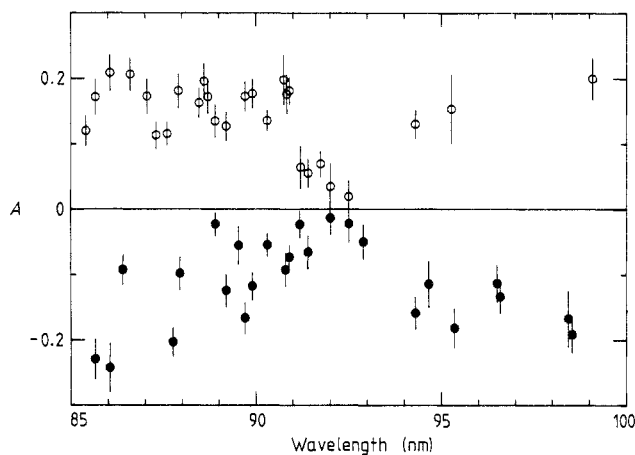


Figure 1. Spin-polarisation parameter A for $\text{HBr}^+ \text{ } ^2\Pi_{3/2} (v=0)$ (open circles) and $\text{ } ^2\Pi_{1/2} (v=0)$ (full circles) final ionic states. The error bars denote the single statistical error including the uncertainty of the Sherman function of the Mott detector and of the light polarisation.

3. Theoretical framework

As described in detail previously (Lefebvre-Brion and Keller 1989), the so-called two-step unified multichannel quantum-defect theory (MQDT) (Giusti 1980, Giusti-Suzor and Jungen 1984), which has been applied to treat simultaneously the autoionisation and predissociation processes in the HCl molecule, is used here for the HBr molecule. The *ab initio* quantities necessary for a MQDT treatment, namely the quantum defects $\mu_{\beta\lambda}$, the transition moments $D_{\beta\lambda}$ and the l -mixing coefficients $U_{l\lambda,\beta\lambda}$ for each $\beta\lambda$ channel, have already been reported for the channels with the $\text{ } ^2\Pi$ ionic core of

HBr⁺ (Lefebvre-Brion *et al* 1986) for an electron energy equal to 0.005 au. The energy region where the autoionised peaks appear corresponds to a slightly larger electron energy but the photoionisation cross section presents a maximum here (Raseev *et al* 1987, figure 3) and we have kept these parameters independent of the electron energy. The corresponding parameters for the A²Σ⁺ ionic core, and the residual electrostatic interaction $V_{\beta\lambda, \beta'\lambda'}^{\Lambda}$ between channels having the same ¹Λ symmetry (here ¹Π and ¹Σ⁺) but belonging to different ionic cores (namely X²Π and A²Σ⁺), are given in table 1. For simplicity, the εfσ and εfπ channels have not been introduced in the final results, owing to their weak contributions. The vibrational overlaps necessary to weight the electronic transition moments or the electrostatic interactions are given in table 2.

The predissociation process has been assumed to be due, as in HCl, to the Rydberg states converging to the a⁴Π repulsive ionic state. The potential curves of these states have been taken parallel to the calculated curve of a⁴Π (Banichevich *et al* 1989). Figure 2 gives the potential curves of this problem. The ³Π₀ with configuration (⁴Π) 5sσ has been assumed to go to the dissociation limit H + Br*(²P_{1/2}, 5s), which occurs at 100.7 nm. Also the (⁴Π) 5pσ state goes to the limit H + Br*(⁴P_{1/2}, 5p), which appears at 94.23 nm. These ³Π₀ states can dissociate only the ¹Σ⁺ states with an A²Σ⁺ core. We have assumed that the ³Σ₁⁺ state with configuration (⁴Π) 5pπ goes to the same

Table 1. *Ab initio* calculated parameters for electronic autoionisation for the A²Σ⁺ ion core ($R = 2.672$ au, $\epsilon = 0.0015$ au).

(a) ¹Π states

| $\beta\lambda$ | $\epsilon p\pi$ | $\epsilon d\pi$ | $\epsilon f\pi$ |
|---|----------------------|----------------------|-----------------|
| $\mu_{\beta\lambda}^0$ | -0.4023 | 0.3191 | 0.0350 |
| | (0.651) ^a | (0.252) ^a | |
| $D_{\beta\lambda}^0$ (au) | 0.9721 | 3.3597 | 0.1760 |
| $U_{\lambda\lambda, \beta\lambda}^0$ | 0.9240 | 0.3804 | 0.0355 |
| | -0.3815 | 0.9115 | 0.1483 |
| | 0.0241 | -0.1560 | 0.9354 |
| $V_{\beta\lambda, \beta'\lambda'}^{\beta\lambda}$ | | | |
| εsσ | -0.0290 | -0.0210 | 0.0032 |
| εpσ | -0.0090 | -0.0581 | -0.0004 |
| εdσ | 0.0244 | 0.0396 | 0.0102 |
| εfσ | -0.0087 | -0.0062 | 0.0046 |
| εdδ | 0.0646 | 0.1076 | -0.0057 |

(b) ¹Σ⁺ states

| $\beta\lambda$ | εsσ | εpσ | εdσ | εfσ |
|---|---------|---------|---------|---------|
| $\mu_{\beta\lambda}^0$ | 0.0176 | 0.4928 | -0.3088 | 0.0461 |
| $D_{\beta\lambda}^0$ (au) | -0.3323 | 0.8194 | 0.0369 | -0.0734 |
| $U_{\lambda\lambda, \beta\lambda}^0$ | 0.7935 | 0.0540 | 0.5075 | 0.1409 |
| | -0.1351 | 0.9740 | 0.1605 | -0.0599 |
| | 0.4524 | 0.2163 | -0.8464 | 0.0522 |
| | 0.2137 | -0.0412 | -0.0168 | -0.9622 |
| $V_{\beta\lambda, \beta'\lambda'}^{\beta\lambda}$ | | | | |
| εpπ | 0.0334 | 0.0361 | -0.0299 | 0.0169 |
| εdπ | -0.0072 | 0.0391 | -0.0619 | -0.0275 |
| εfπ | 0.0034 | -0.0049 | -0.0287 | -0.0005 |

^a Values in parentheses are the values used in the calculations.

Table 2. Vibrational quantities for the $A^2\Sigma^+$ state of HBr^+ ^a.

| v' | ΔG (cm^{-1}) | $\langle v' X^1\Sigma^+ (v''=0)\rangle$ | $\langle v' X^2\Pi (v''=0)\rangle$ |
|------|---------------------------------|---|------------------------------------|
| 0 | 1328.0 | 0.3412 | 0.4549 |
| 1 | 1253.0 | 0.4552 | 0.5271 |
| 2 | 1177.0 | 0.4630 | 0.4716 |
| 3 | 1102.0 | 0.4131 | 0.3740 |
| 4 | 1026.0 | 0.3419 | 0.2774 |
| 5 | 951.0 | 0.2702 | 0.1980 |
| 6 | 875.0 | 0.2078 | 0.1383 |
| 7 | | 0.1573 | 0.0956 |

^a Parameters for Morse potentials (from Huber and Herzberg 1979):HBr $X^1\Sigma^+$

$$\omega_e = 2648.975 \text{ cm}^{-1} \quad \omega_e x_e = 45.217 \text{ cm}^{-1} \quad r_e = 1.41443 \text{ \AA}$$

 $\text{HBr}^+ X^2\Pi$

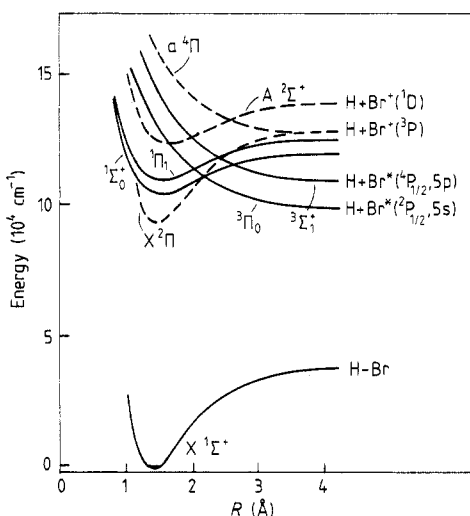
$$\omega_e = 2441.52 \text{ cm}^{-1} \quad \omega_e x_e = 47.4 \text{ cm}^{-1} \quad r_e = 1.4484 \text{ \AA}$$

$$\text{IP} = 94130 \text{ cm}^{-1} \text{ for } X^2\Pi_{3/2} \quad \text{IP} = 96781 \text{ cm}^{-1} \text{ for } X^2\Pi_{1/2}$$

 $A^2\Sigma^+$

$$\omega_e = 1404 \text{ cm}^{-1} \quad \omega_e x_e = 37.75 \text{ cm}^{-1} \quad r_e = 1.6842 \text{ \AA}$$

$$\text{IP} = 29230 \text{ cm}^{-1}$$

**Figure 2.** Experimental potential curves of the bound states of HBr and HBr^+ . The $^4\Pi$ repulsive curve of HBr^+ is taken from calculations of Banichevich *et al.* (1989). The curves for Rydberg states are taken parallel to the curve of their ionic core.

limit as the last $^3\Pi_0$ state. It can predissociate the $^1\Pi$ states. For simplicity, we have not considered the limit $\text{H} + \text{Br}^*(^4D_{1/2}, 5p)$ at 92.27 nm, which can contribute very much to the dissociation of the $nd\pi^1\Pi$ states, and the effect of the lowest $^3\Pi_0$ has been taken into account only up to the second dissociation limit, namely 94.23 nm. The highest dissociation limit included in this study is reported on figure 3. The spin-orbit interaction between the $^3\Pi$ state (with a $^4\Pi$ core) and the $^1\Sigma^+$ state (with $A^2\Sigma^+$ core) is four times larger than in HCl (as the splitting between the cores $X^2\Pi$) and is equal to 2080 cm^{-1} for HBr as compared to 520 cm^{-1} for HCl (Lefebvre-Brion and Keller 1989).

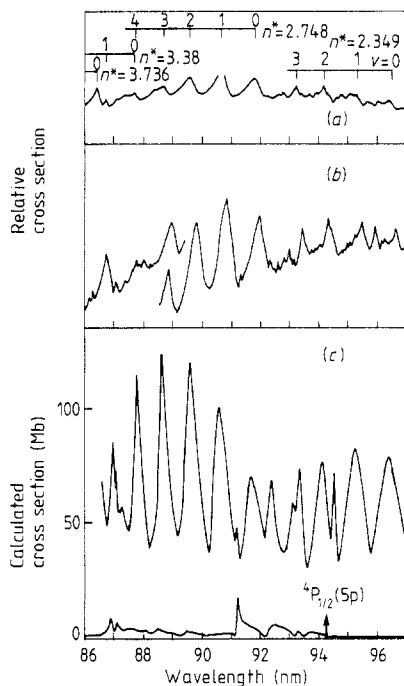


Figure 3. (a) Experimental photoionisation cross section with a resolution of 0.14 Å (Dehmer and Chupka 1978). (b) Experimental photoabsorption cross section with a resolution of 0.04 Å (Terwilliger and Smith 1974). (c) Calculated photoionisation (top) and photodissociation cross sections (bottom).

The photoelectron angular distribution parameter β and the spin-polarisation parameter A were calculated from the transition moments.

4. Theoretical results and comparison with experiment

Figure 3 reports both the calculated photoionisation and photodissociation cross sections. The photoionisation cross section compares rather well with the experimental cross sections for photoabsorption (Terwilliger and Smith 1974, 1975) and photoionisation (Dehmer and Chupka 1978), after the quantum defects of the $^1\Pi$ states have been slightly modified to fit the peak positions in the photoionisation cross section (see table 1). It is seen that the most intense autoionisation peaks have the $^1\Pi$ symmetry and are $5p\pi$ (progression II of Terwilliger and Smith 1975) and $4d\pi$ (progression I). The calculated photodissociation cross section is due mainly to the $^1\Sigma^+$ states, here the $4d\sigma$ state. It is predicted to culminate at about 10 Mb, i.e. an order of magnitude larger than in HCl, as predicted (Lefebvre-Brion and Keller 1989). These results depend strongly on the quantum defects of the $^1\Sigma^+$ states, which have been taken from the calculation, and on the shape of the predissociating states, and comparison with experimental results would be very interesting. From the comparison between experiment and calculation of the relative intensity of the peaks of the $5d\pi$ progression, it is possible that the $5d\pi$ state be strongly predissociated. It would be necessary in our model to include the dissociative state going to the $H + Br^*(^4D_{1/2}, 5p)$ limit. The

photoelectron angular distribution parameter β has been calculated with and without including predissociation (see figures 4(a) and (b)). As expected, the influence of predissociation of the $4d\sigma$ state can be seen in the 94–91 nm wavelength region as a small variation. Note that the calculations have been made with the transition moments calculated for $\varepsilon = 0.005$ au. If the calculations are made with the transition moments calculated for the actual value of ε , we estimate that σ would be practically unchanged and β would increase by about 20%. The strong variation of β observed in this energy domain (Raseev *et al* 1987) is due mainly to the energy dependence of the Coulomb phaseshift. For comparison with the structures predicted in figure 4, it would also be interesting to perform measurements of the parameter β . However, the influence of the predissociation on β as calculated in the energy region considered is too small to be detected experimentally.

Calculations have also been performed including only the $v = 0$ level of $X^2\Pi$. The electrostatic interactions between the $A^2\Sigma^+$ and the $v = 0$ $X^2\Pi$ channel have been weighted by the vibrational overlap given in the fourth column of table 2. With these results, the A (or \bar{P}) spin-polarisation parameter has been calculated (see figure 5) for $v = 0$ of $X^2\Pi_{1/2}$ in order to compare with the experimental data. Note that its value is given for the $X^2\Pi_{1/2}$ substate by the formula (Raseev *et al* 1987, equation (31))

$$\bar{P}(1/2) = A(1/2) = (\sigma_{\Pi}^{\sigma} - \sigma_{\Pi}^{\delta}) / (2\sigma_{\Pi}). \quad (2)$$

Thus the contribution to A (or \bar{P}) of the autoionisation peaks in the numerator of equation (1) comes only from the $^1\Pi$ states, which are autoionised either in the ($X^2\Pi$)

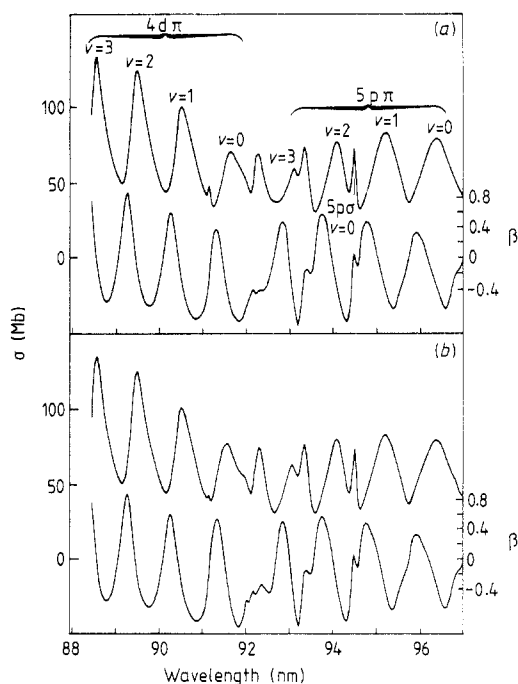


Figure 4. (a) Calculated photoionisation cross section, with predissociation (top) and calculated photoelectron angular distribution parameter β , with predissociation (bottom). (b) Calculated photoionisation cross section, without predissociation (top) and calculated photoelectron angular distribution parameter β , without predissociation (bottom).

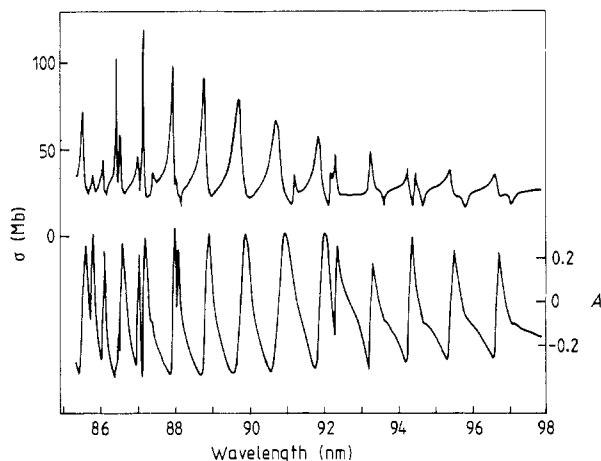


Figure 5. Calculated photoionisation cross section, without predissociation, for $v=0$ of $X^2\Pi_{1/2}$ (top) and calculated spin-polarisation parameter A (bottom).

$\epsilon\sigma$ or ($X^2\Pi$) $\epsilon\delta$ continua of $^1\Pi$ total symmetry (see table 1). Since the experimental results of A in this energy region show a deviation from the calculated smooth curve without autoionisation, this is indirect proof that the autoionised peaks are mainly of $^1\Pi$ symmetry.

In figure 6, the experimental results (see figure 1) are compared to the calculated results convoluted to a resolution of 500 cm^{-1} . Since in general relation (1) was verified, we show in figure 6 $A(1/2)$ and $-A(3/2)$. Qualitative agreement is found between theory and experiment. In particular, owing to the inclusion of electronic autoionisation, the theoretical results correctly predict a deviation of A from the calculated value of about -0.2 for the open continuum (Raseev *et al* 1987). This is also observed in the experiment.

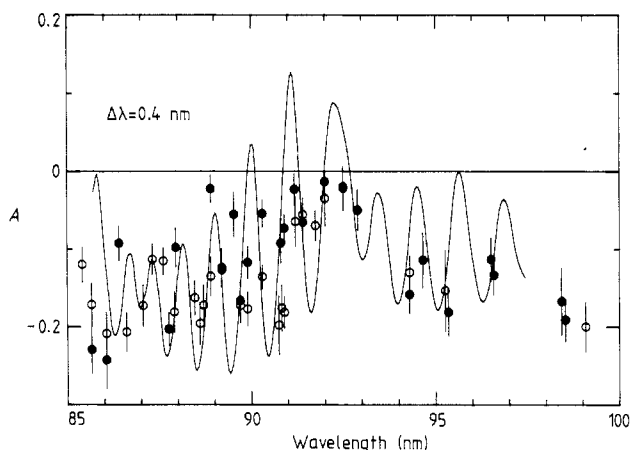


Figure 6. Calculated spin-polarisation parameter A convoluted to the resolution of 500 cm^{-1} in comparison with the experimental data. The data points shown are $A(1/2)$ (full circles) and $-A(3/2)$ (open circles).

The experimental data at the present stage are not sufficiently dense to outline completely the wavelength dependence of A in full detail; however, a strong variation in the photon energy range examined is clearly indicated. A comparison of the individual photon data points with the theoretical prediction can be made: most of them lie on or close to the theoretical curve, although some deviations do exist. The convolution of the calculated curve for A to the experimental resolution caused the amplitude of the oscillations to decrease (as can be seen from a comparison of figure 6 with figure 5, where A is shown without convolution). The oscillatory shape seems to be more distinct in the calculation than experimentally observed. However, in the photoionisation cross section (see figure 3), the ratio of the oscillation amplitude to the background appears to be too large in the calculation when compared to the experimental results. Since A is a ratio of partial cross sections, this could in part explain why the experimentally observed oscillations for A are less pronounced than calculated.

The cause of the oscillatory shape for A is illustrated in figure 7 where the partial contributions σ_{Π}^{σ} and σ_{Π}^{δ} are plotted as a function of energy. They oscillate with different phases and consequently it can be understood why A is also an oscillating function of energy. From figure 7 it can also be comprehended why the theory predicts the structures for A to be slightly shifted in wavelength compared to the partial cross section: to calculate the parameter $A(1/2)$, the partial contribution σ_{Π}^{δ} has to be subtracted from σ_{Π}^{σ} according to equation (2), whereas in order to calculate the cross section the partial contributions have to be added.

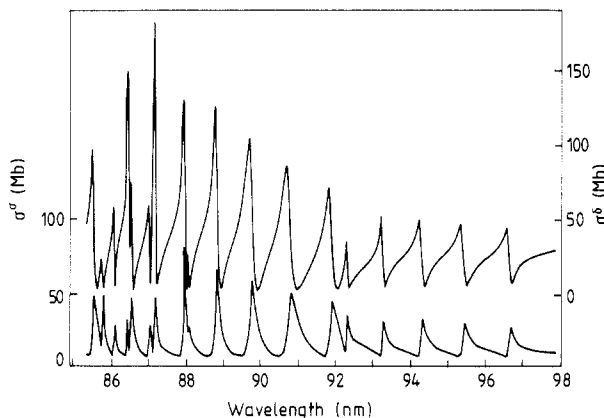


Figure 7. Values of σ_{Π}^{σ} (bottom) and σ_{Π}^{δ} (top) as a function of energy.

5. Conclusions

In conclusion, the results illustrate the necessity to include the influence of autoionisation and predissociation in the calculation and interpretation of the experimental findings. Further, experiments would be very useful in order to verify the theoretical predictions both for the dissociation cross sections and for the β parameter. For the spin-polarisation parameter A , more extensive experiments are planned. Measurements for A were also made for the HI molecule (Böwering *et al* 1989). Unfortunately, for this molecule, the width of the resonances is of the order of magnitude of the vibrational

interval and it would be necessary to modify the theory used here by the introduction of coupled equations.

Acknowledgments

One of the authors (HLB) thanks F Keller for useful discussions, G Raseev and H Le Rouzo for making available their program for the calculation of the *ab initio* parameters. The other authors would like to thank the BESSY staff, in particular F Schäfers, for cooperation and acknowledge support by BMFT (05 331 and 437 AXI). We thank S Peyerimhoff and A Banichevich for sending the calculated potential curves of HBr^+ prior to publication. This joint research was supported by the European Commission.

References

- Banichevich A, van Hemert M C and Peyerimhoff S 1989 to be submitted
- Böwering N, Huth T, Mank A, Müller M, Schönhense G, Wallenstein R and Heinzmann U 1988 *Electron-Molecule Scattering and Photoionisation* ed P G Burke and J B West (New York: Plenum) pp 139-46
- Böwering N, Müller M, Salzmann M, Klausning H W and Heinzmann U 1989 to be published
- Cherepkov N A 1981 *J. Phys. B: At. Mol. Phys.* **14** 2165-77
- Dehmer P M and Chupka W A 1978 *Argonne National Laboratory Report* ANL-78-65, part I, pp 13-18
- Frohlich H, Glass-Maujean M and Guyon P M 1989 *J. Chem. Phys.* to be submitted
- Giusti A 1980 *J. Phys. B: At. Mol. Phys.* **13** 3867-94
- Giusti-Suzor A and Jungen Ch 1984 *J. Chem. Phys.* **80** 986-1000
- Heckenkamp Ch, Schäfers F, Schönhense G and Heinzmann U 1986 *Z. Phys. D* **2** 257-74
- Heinzmann U, Osterheld B, Schäfers F and Schönhense G 1981 *J. Phys. B: At. Mol. Phys.* **14** L79-84
- Heinzmann U, Schäfers F and Hess B A 1980 *Chem. Phys. Lett.* **69** 284-9
- Huber K P and Herzberg G 1979 *Molecular Spectra and Molecular Structure* vol IV *Constants of Diatomic Molecules* (New York: Van Nostrand-Reinhold)
- Jost K 1979 *J. Phys. E: Sci. Instrum.* **12** 1006-12
- Lefebvre-Brion H, Dehmer P M and Chupka W A 1986 *J. Chem. Phys.* **85** 45-50
- 1988 *J. Chem. Phys.* **88** 811-17
- Lefebvre-Brion H and Keller F 1989 *J. Chem. Phys.* **90** 7176-83
- Raseev G, Keller F and Lefebvre-Brion H 1987 *Phys. Rev. A* **36** 4756-74
- Schäfers F, Peatman W, Evers A, Heckenkamp Ch, Schönhense G and Heinzmann U 1986 *Rev. Sci. Instrum.* **57** 1032-41
- Terwilliger D T and Smith A L 1974 *J. Mol. Spectrosc.* **50** 30-7
- 1975 *J. Chem. Phys.* **63** 1008-20
- White M G, Leroi G E, Ho M H and Poliakoff E D 1987 *J. Chem. Phys.* **87** 6553-8